Available online www.jocpr.com

Journal of Chemical and Pharmaceutical Research, 2015, 7(4):1500-1511

Research Article

ISSN : 0975-7384
CODEN(USA) : JCPRC5

Factorial design of experiment model enables to optimize the variables in wastewater decolorization process by using areca husk activated carbon fibre

A. Basker[1*] and P. S. Syed Shabudeen[2]

[1]*Department of Chemistry, Kalaignar Karunanidhi Institute of Technology, Coimbatore, Tamil Nadu (India)*
[2]*Department of Chemistry, Kumaraguru College of Technology, Coimbatore, Tamil Nadu (India)*

ABSTRACT

The factorial experimental design technique has been used to investigate the adsorption of Bismarck Brown-Y (BBY) from wastewater onto agricultural waste Areca Husk Carbon Fibre (AHCF). The Factorial Design (2^3) is adopted for optimizing variable parameters from these studies. The interaction between three process parameters for the adsorption of dye is optimized. Batch mode of experiments is carried out for the adsorption studies. The adsorption parameters pH, temperature and particle size of the adsorption capacity are analysed and optimized as pH 4-9, particle size 100-250 BSS and temperature 300-320 K. The statistical tools t-test, ANOVA, F-test are tested to verify the fitness of adsorption and the results are validated by this design of experimental model. All these values revealed with the normal probability plots, main & interaction plots, Pareto charts and contour plots. The regression values are evolved with Design of Experiment software and prove the fitness on experimental data. Physico-Chemical characteristics and adsorption efficiency of AHCF of the wastewater are also determined and the results revealed AHCF is a good adsorbent. The structural and morphological features of activated carbon are characterized by FTIR, XRD, SEM and EDAX studies.

Key words: Areca Husk Activated Carbon Fibre, Bismarck BrownY, Factorial Design, ANOVA.

INTRODUCTION

The major flow process chemical industries using water and discharging effluents are textile processing, Kraft bleaching, food stuff production units etc., are considered for a wide variety of organic pollutant loads. In which synthetic dyes are introduced into the natural water resources and discharged as wastewater and these effluents are directly fed into various receiving bodies including ponds, rivers and other public sewer without any treatment process. As a result, they generate a considerable amount of coloured wastewaters negative influence for its portability. The public perception of water quality is greatly influenced by the colour developed due to these types of synthetic dyes which are harmful to humans and animals. It is the first contaminant and its presence in small amounts of dyes in effluent is highly visible and undesirable [1]. The toxic wastes and non-biodegradable pollutants present in water bodies threatening the ecosystem have caused great concern among the ecologists [2]. Textile industry causes considerable higher impacts of water receiving bodies have been adversely affected in their physical, chemical, biological and microbiological characteristics of water quality according to the standards (WHO). Major pollutant load from the textile industries are from the several of their wet-processing operations like scouring, bleaching, mercerizing and dyeing [3]. Among these various processes, dyeing process normally uses large amounts of water for dyeing, fixing and washing processes [4]. Thus, waste water contains large amounts of suspended solids, strong colour, pH, high temperature and low biodegradability caused by varying contaminates within the water environment [5]. Hence, their removal from aquatic wastewater becomes environmentally most important [6]. This makes treating water contamination difficult, because the colour tends to persist even after the conventional processes [7]. The dye contaminations in water tend to prevent light penetration and therefore, affect the

photosynthesis activity [8-10]. Due to the wide application of dye compound and their numerous hazard and toxic derivatives, the cleaning of wastewater from colour dyestuff becomes primarily an important issue [11].

EXPERIMENTAL SECTION

Preparation of Areca Husk Carbon Fibre

One part by weight of each powdered raw material is chemically activated by treating with two parts by weight of concentrated sulphuric acid with constant stirring and is kept for 24 hours in a hot air oven at 75^{o}C, the carbonized material is washed well with plenty of water several times to remove excess acid, surface adhered particles, water soluble materials dried at 200^{o}C in hot air oven for 24 hours. The adsorbent thus obtained are grounded well and kept in air tight containers for further use.

Analysis of Bismarck Brown Y

BBY supplied by Sigma–Aldrich (M) Sdn Bhd, Malaysia is used as an adsorbate and is not purified prior to use. Distilled water is employed in preparing all the solutions and reagents. The concentration of BBY in the supernatant solution after and before adsorption is determined using a double beam UV spectrophotometer (Shimadzu, Japan) at 516 nm. It is found that the supernatant from the activated carbon did not exhibit any absorbance at this wavelength and also that the calibration curve is very reproducible and linear over the concentration range used in this work.

Batch equilibrium studies

BBY dye solutions are prepared with distilled water. Batch experiments are carried in a glass beaker by shaking a fixed mass of AHCF (200 mg) with 100ml diluted solution (20 mg/L) at 1200 rpm. After agitation the dye solution centrifuged. Then the dye concentration in the supernatant solution is analyzed using a spectrophotometer by monitoring the absorbance changes at a wavelength of maximum absorbance (516nm) in these sorption experiments. Each experiment is carried out in duplicate and the average results are presented. Calibration curves are obtained with standard BBY solution using distilled water as a blank. Adsorption capacity is calculated from the difference between the initial and the final concentration of BBY in solution.

$$q_e = \frac{(C_o - C_e)}{W} \quad (1)$$

Where C_0 and C_e (mg/L) are the liquid-phase concentrations of dye at initial and equilibrium respectively. V is the volume of the solution (l), and W is the mass of dry adsorbent used (g).

RESULTS AND DISCUSSION

Characteristics of Areca Husk Carbon Fibre

It is a unique fact that the material selected for water treatment process should fulfill the mandatory quality requirements and should fulfill the norms laid down by the World Health Organization. These quality parameters can only be identified by characterization of the material chosen for the treatment process. Keeping the core idea to select the Areca Husk Carbon Fibre as an adsorbent, the characteristic studies are performed and inferred that, about 2.4% of moisture is contained in it. This will not influence the adsorptive power of activated carbon. It has been observed that if the moisture content of the adsorbent is more, it will dilute the action of activated carbon and it is utilizing some extra load of carbon. The activation process of AHCF by adopting 1:1 Sulphuric acid treatment leads to create a surface of carbonaceous material with the introduction of micro, macro and mesopores [12].

If the fixed carbon content of the adsorbent is nearly 80% this results in low ash content and from the analysis, it is inferred that a low ash content of 1.2% [13] and a high 83.47% of fixed carbon. From the solubility studies, the presence of impurities can be detected and these impurities will affect the quality of the treated water. It is observed that the AHCF contains only the permitted level of impurities. The incorporation of acid in the carbon structure [14] makes it into acidic (pH 6.3) and with very little ion exchange capacity. The characterization of this activated carbon shows that the iron content is very minimal and the leaching problem of iron in treating water is satisfactorily ruled out. The phenol adsorption capacity and decolourizing power are 11.2 and 22.6 mg/g, respectively, which indicates that the carbon prepared by acid activation method has the very good adsorption capacity and it can be considered for adsorption of organic dyes.

The BET surface area of AHCF is found to be 310.2 m^2/g and it is comparable to various low cost adsorbents namely Coconut husk carbon - 296 m^2/g [15], Eucalyptus kraft lignin char - 496 m^2/g [16], Tea leaf carbon - 366 m^2/g [17], Grape seeds - 487 m^2/g [18], Cashew nut shell carbon - 269 m^2/g, MgO Nanoplates - 198 m^2/g [19], Palm Shell - 477 m^2/g [20], Sepiolite Clay - 340 m^2/g [21].

Table 1 Characteristics of Areca Husk Carbon Fibre

S. No	Parameters	Obtained Results
1	pH	6.3
2	p^{H}_{zpc}	6.0
3	Carbon (%)	83.47
4	Oxygen (%)	15.83
5	Sodium (%)	0.20
6	Aluminium (%)	0.27
7	Sulphur (%)	0.08
8	Chloride (%)	0.04
9	Potassium (%)	0.03
10	Calcium (%)	0.08
11	Moisture content (%)	2.4
12	Ash content (%)	1.2
13	Decolourizing power (mg/g)	22.6
14	Ion-exchange capacity (meq/g)	0.042
15	BET Surface area (m^2/g)	310.2
16	Pore size (nm)	5.43
17	Pore volume (mL/g)	0.12
18	Bulk density (g/L)	0.42
19	Water soluble matter (%)	2.1
20	Acid soluble matter (%)	7.3
21	Phenol number	11.2

SEM Morphology

From this study the surface pores have been identified and shows a uniform distribution. The SEM images are shown in fig.1 revealed that the AHCF has a rough and uneven surface with more porous, it seems to be caves like structure. The distribution of these pores in the activated carbons is varied significantly depending upon the raw materials utilized for the preparation. Various shapes of these pores with the different of raw materials are already reported. The efficiency and selectivity of adsorption depend upon the nature and distribution of pore volume. A consideration of the dimensions of some pollutants shows that activated carbon can feasibly be used to remove many of the impurities occurring in water. The higher resolution of the images under magnification shows the nature of pores build-up is found to be with very clear openings with rough surface area. This character of the adsorbent provides an accessibility of the adsorbate into the internal adsorption sites namely pores with high surface area that serve the purpose of the adsorption phenomenon.

From fig. 2 shows energy dispersive analysis (EDAX) has been used for the characterization of adsorbent and to elucidate the probable mechanism of adsorption. This study infers the presence of carbon, oxygen and trace amounts of sodium, aluminium, silicon, sulphur, chloride, potassium and calcium.

The SEM images of AHCF loaded with BBY are shown in fig. 3 which show the surface of the adsorbent is saturated with the adsorption of the various dye molecules. The surface modifications due to the adsorption of these adsorbents are identified and presumably leading to the formation of a monolayer of the dye molecules over the adsorbent surface. This is evident from the formation of the white layer in the loaded carbon. A close scrutiny of SEM images infers the discovery about the density differences before and after the adsorption of various dyes onto AHCF. This confirms the uptake of dye molecules from the wastewater.

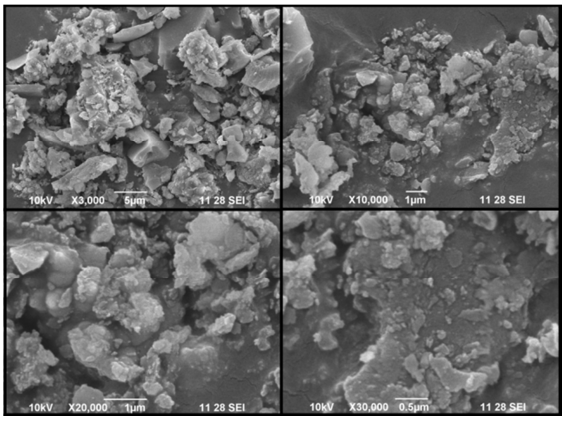

Fig. 1 SEM image of Fresh Areca Husk Carbon Fibre (AHCF)

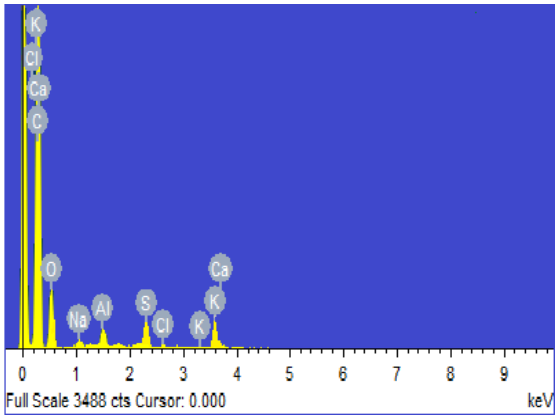

Fig. 2 EDAX image of Fresh AHCF

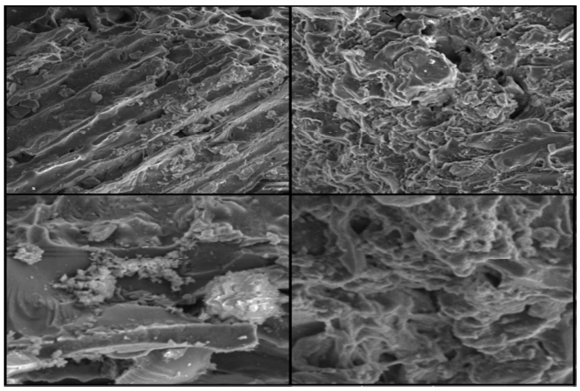

Fig. 3 SEM image of BBY loaded AHCF

FTIR Studies

The FT-IR spectrum of BBY onto AHCF before and after adsorption is detected in the range of 4000 to 400 cm^{-1} is presented in Figs. 4 and 5. The band observed in 3425.58cm^{-1} is assigned to a ν (O-H) stretching vibration. The absorption band at 2854.65aa and 2924.09cm^{-1} can be attributed to the stretching vibrations of ν(C-H) bonds in alkane and alkyl groups where carbon is bonded with hydrogen bonds. Adsorption bands at 2337.72 and 2376.30cm^{-1} are corresponds to ν (N-H) stretching. The band at 1573.91cm^{-1} shows the asymmetry ν (COO-) stretching. The band at 1450.47cm^{-1} may be attributed to the aromatic ν(C=C) stretching vibration. At 1111.00cm^{-1}, the band is highly intense ν(C-O) and is related to the ν(C-O) stretching vibration of the bonds in ester, ether, or phenol groups. The band corresponding to 802.39cm^{-1} in the fingerprint area indicates a mono substituted aromatic structure. The weak absorption band at 678.94cm^{-1} corresponds to the ν(O-H) vibration in the benzene ring. The band at 462.92 and 594.08cm^{-1} which are associated with the in-plane and out-of plane aromatic ring deformation vibrations common that is quite common for activated carbon.

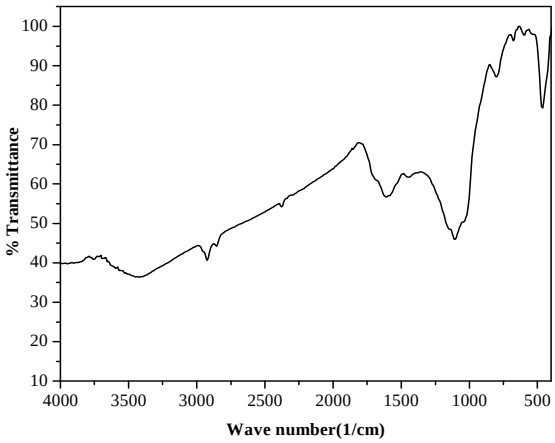

Fig. 4 FTIR spectra of fresh AHCF

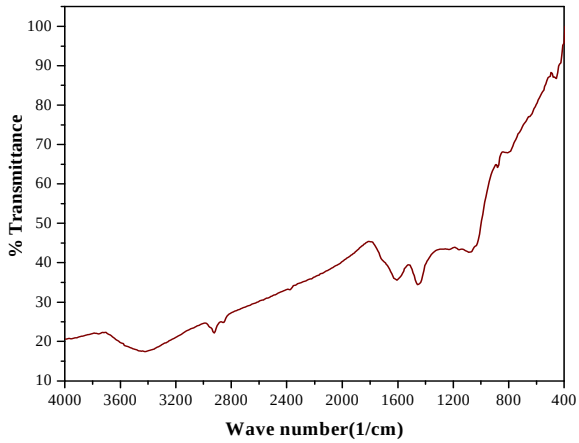

Fig. 5 FTIR spectra of BBY loaded AHCF

The result shows that BBY onto AHCF possessed more carboxyl groups than the unabsorbed AHCF. These groups functioned as proton donors and deprotonated hydroxyl and carboxyl groups and it may be involves in coordination with positive dye ions during adsorption. Dissolved BBY ions are positively charged and will undergo attraction on approaching the anionic AHCF structure. On this basis, it is expected that AHCF will show a strong sorption affinity towards BBY ions. In addition, some of the peaks are disappeared due to the absorption of BBY on AHCF.

X ray diffraction studies

Crystalline nature of the material is determined through an efficient technique known as X-ray diffraction. If the material under investigation is crystalline, well defined peaks are observed while non-crystalline or amorphous systems show hallow instead of well defined peak [22]. The XRD pattern of unloaded AHCF is crystalline in nature and shows sharp peaks corresponding with 2Θ = 21.2, 23.7 and 26.0 are shown in the Fig. 6 [23]. The XRD pattern of AHCF loaded with various dyes is slightly hanging peaks when compared to unloaded AHCF as shown in the Fig.7. This suggests that the dye molecules diffuse into micropores and mesopores areas of adsorption. The nature of physisorption and partially by chemisorption with altering the structure of the carbon has already been reported [24]. The studies on the effect of pH and desorption indicates the nature of the adsorption [25]. The XRD study shows the

changes in the crystalline nature of the adsorbent due to the accumulation of dye molecules during the process of adsorption.

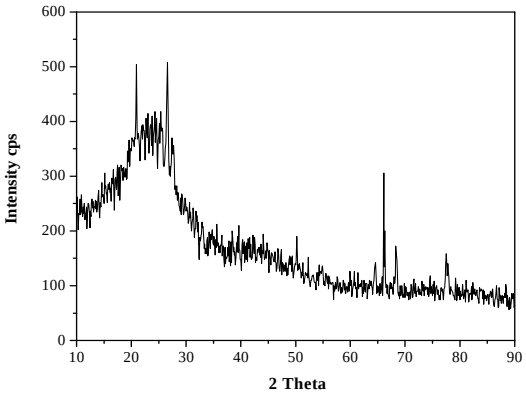

Fig. 6 XRD spectrum of fresh AHCF

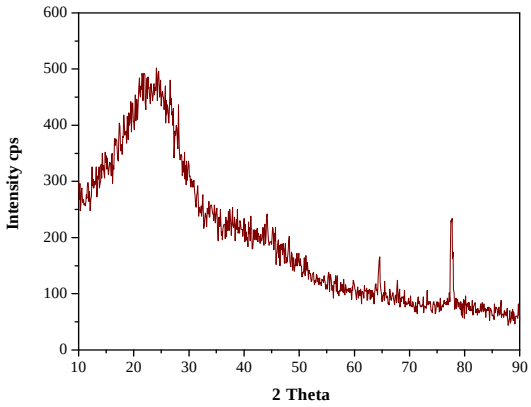

Fig. 7 XRD spectrum of BBY loaded AHCF

Factorial Experimental Design (FED)

Factorial design is employed to reduce the total number of experiments in order to achieve the best overall optimization of the system [26]. It is used to reduce the number of experiments, time, overall process cost and to obtain a better response [27].

The design determines that factors have important effects on a response as well as how the effect of one factor varies with the level of the other factors. The number of experimental runs at b levels is back, where k is the number of factors [28]. Today, the most widely used kind of experimental design, to estimate the main effects as well as interaction effects, is the 2K factorial design in which each variable is investigated at two levels [29]. If the total numbers of factors are known, it is immediately possible to find the number of trial experiments needed for realization in all possible combinations by using the simple formula:

$$N = 2^k \quad (2)$$

Where, N is the number of trial experiments, K is the number of factors varies and 2 is the number of levels. The high and low levels defined for the 2^3 factorial designs are listed in Table 2. The low and high levels of the factors are selected according to some preliminary experiments [30]. The factorial design matrix and adsorption capacity is measured in each factorial experiment is listed in table3 with the low (−1) and high (+1) levels [31]. Adsorption capacity is determined as the average of three parallel experiments. The order in which the experiments are made is randomized to avoid systematic errors. The main effects and interactions between factors are determined. From figs. 9 and 10 illustrated the mean of the experimental results for the respective low and high levels of pH, Particle Size and temperature. The results are analysed and along with the main effects the interactions of different factors are determined. The regression equation for the matrix is represented by the following expression [32].

$$q_e = X_0 + X_1A + X_2B + X_3C + X_4AB + X_5BC + X_6AC + X_7ABC \quad (3)$$

Where q_e is the adsorption capacity of dyes, X_0 is the global mean, X_i represents the other regression coefficients and A, B, C stands for pH, temperature and Particle Size respectively. Once the experimental levels are chosen, the condition can be mentioned in the form of a table with rows and columns, where the rows correspond to different trials and columns as values of the factors. Such a representation is called experimental by designed matrix. Here, each column is termed as column factor and row factors as shown in Table 3.

Table 2 Factors and levels used in the factorial design

Factor Coded	Symbol	Low Level (-1)	High Level (+1)
pH	A	4	9
Particle Size	B	100	250
T(K)	C	300	320

Factors that influence the quantity of dye adsorbed by AHCF are evaluated by using factorial plots: main effect, interaction effect, the Pareto chart plot, normal probability plots and the contour plot. ANOVA and P-value

significant levels are used to check the significance of the effect on q_e. The main effect and interactions are also observed in the Pareto chart plot.

Table 3 Design matrix of an 8 run experiment with 3 factors

Trial No.	Coded values of independent variables			Coded values of interaction variables			
	pH (A)	PS (B)	Temp (C)	AB	BC	AC	ABCs
1	-1	-1	-1	1	1	1	-1
2	1	-1	-1	-1	1	-1	1
3	-1	1	-1	-1	-1	1	1
4	1	1	-1	1	-1	-1	-1
5	-1	-1	1	1	-1	-1	1
6	1	-1	1	-1	-1	1	-1
7	-1	1	1	-1	1	-1	-1
8	1	1	1	1	1	1	1

Table 4 Analysis of Variance for q_e (coded units) for BBY adsorption

Source	DF	Adj SS	Adj MS	F-Value	P-Value
Model	7	0.639312	0.09133	101.55	0
Linear	3	0.615743	0.205248	228.21	0
pH	1	0.07122	0.07122	79.19	0
T(K)	1	0.387057	0.387057	430.37	0
P.S(BSS Mesh)	1	0.155189	0.155189	172.55	0
2-Way Interactions	3	0.005016	0.001672	1.86	0.171
pH*T(K)	1	0.000462	0.000462	0.51	0.482
pH*P.S(BSS Mesh)	1	0.000185	0.000185	0.21	0.655
T(K)*P.S(BSS Mesh)	1	0.004337	0.004337	4.82	0.041
3-Way Interactions	1	0.000005	0.000005	0.01	0.94
pH*T(K)*P.S(BSS Mesh)	1	0.000005	0.000005	0..01	0.94
Error	19	0.017088	0.000899		
Total	26	0.6564			

Analysis of Variance (ANOVA)

After estimating the main effects, the interacting factors affecting the removal of various cationic dyes Such as Bismarck Brown onto AHCF are determined by performing the analysis of variance (ANOVA).

Table 5 Estimated Effects and Coefficients for q_e (coded) for BBY adsorption

Term	Effect	Coef	SE Coef	T-Value	P-Value	VIF
Constant		8.49605	0.00584	1454.33	0	
pH	0.12608	0.06304	0.00708	8.9	0	1.02
T(K)	0.29686	0.14843	0.00715	20.75	0	1.02
P.S(BSS Mesh)	0.18296	0.09148	0.00696	13.14	0	1.01
pH*T(K)	-0.01244	-0.00622	0.00868	-0.72	0.482	1.02
pH*P.S(BSS Mesh)	-0.00767	-0.00383	0.00845	-0.45	0.655	1.02
T(K)*P.S(BSS Mesh)	-0.03746	-0.01873	0.00853	-2.2	0.041	1.02
pH(K)*P.S(BSS Mesh)	0.0016	0.0008	0.0103	0.08	0.94	1.02

It is a statistical technique that subdivides the total variation in a set of data into component parts associated with specific sources of variation for the purpose of testing hypotheses on the parameter of the model [33]. Sum of squares (SS) of each factor quantifies its importance in the process and as the value of the SS increases the significance of the corresponding factor in the undergoing process also increases (Tables 4 & 5). The main and interaction effects of each factor having P values < 0.05 are considered as potentially significant [34]. From table 4 and 5 shows the sum of squares being used to estimate the factors effect and the F-ratios, which are defined as the ratio of respective mean square effect to the mean square error.

The significance of these effects is evaluated using the t-test, and has a significance level of 5 % with a confidence level of 95%. The R-squared statistic indicated that the first-order model explained 100 % of R^2 variability to the rejection of the null hypothesis, it appears that the main effect of each factor and the interaction effects are statistically significant: P<0.05 [35]. The results revealed that the studied factors (A, B and C), their 2-way interaction (AB, AC and BC) and 3-way interaction (ABC) are statistically significant to adsorption capacity (q_e).
In this way, the dye uptake by AHCF could be expressed using the following equation:

$$q_e = 1.49 + 0.129\ A + 0.02131\ B + 0.0099\ C - 0.000322\ AB - 0.00015\ AC - 0.000028\ BC + 0.000000\ ABC$$

Table 6 Experimental and theoretically predicted Factorial Design values

pH	Temp	Particle Size	Predicted	Observed	Residual
4	300	100	12.438	12.451	-0.014
4	310	100	12.474	12.478	-0.004
4	320	100	12.491	12.504	-0.013
4	300	150	12.512	12.499	0.013
4	310	150	12.545	12.524	0.021
4	320	150	12.562	12.549	0.012
4	300	250	12.587	12.595	-0.008
4	310	250	12.617	12.617	0.000
4	320	250	12.632	12.639	-0.007
7	300	100	12.464	12.477	-0.013
7	310	100	12.499	12.503	-0.004
7	320	100	12.516	12.529	-0.013
7	300	150	12.536	12.523	0.013
7	310	150	12.568	12.548	0.020
7	320	150	12.584	12.572	0.012
7	300	250	12.609	12.616	-0.008
7	310	250	12.638	12.638	0.000
7	320	250	12.652	12.659	-0.007
9	300	100	12.481	12.494	-0.013
9	310	100	12.515	12.519	-0.004
9	320	100	12.532	12.545	-0.012
9	300	150	12.552	12.540	0.013
9	310	150	12.583	12.564	0.020
9	320	150	12.599	12.587	0.012
9	300	250	12.623	12.631	-0.007
9	310	250	12.652	12.652	0.000
9	320	250	12.666	12.673	-0.007

Effect of Cube plots

Cube plots visualized the average response values at all combinations of process design and parameter settings. One can easily determine the best and unfavourable combinations of factor levels for achieving the desired optimum response. A cube plot is useful to define the path of steepest ascent or descent for optimization problems. From the fig. 8 illustrates of cube plot for adsorption optimization study with three optimization parameters (pH, particle size and temperature). The graph indicates that adsorption increases when the three parameters set at high levels (+1). The worst condition occurs when all factors are set at low levels (-1). From the above result, we determine the best factor setting which remove the maximum dye from the wastewater.

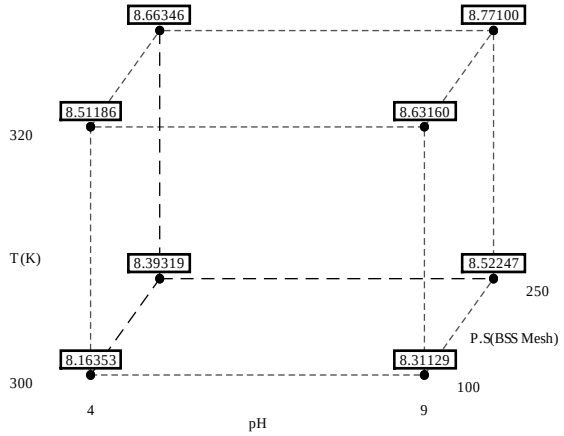

Fig. 8 Cube plot for BBY adsorption

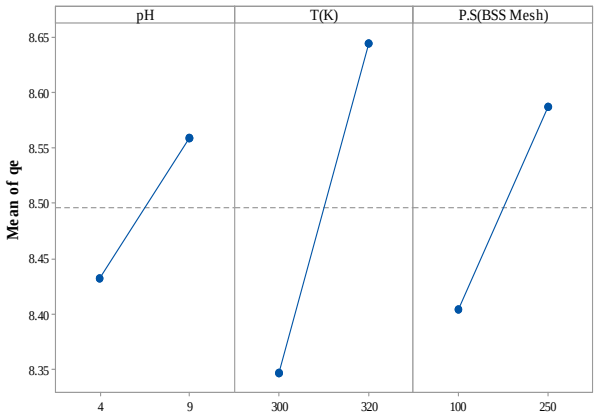

Fig. 9 Main plot for BBY adsorption

Effect of Main and Interaction effects

The experiments are performed at the specified combinations of the physical parameters using statistically designed experiments in order to study the combined effects of these factors. The main effects are analyzed by adsorption of BBY onto AHCF the experiments are conducted at different pH (4, 7 and 9), Particle size (100, 150 and 250 BSS Mesh) and Temperature (300, 310 and 320K). The main effects of all the variables taken into consideration in this work are presented in fig. 9. The effect of each factor is statistically significant at $P < 0.05$ for AHCF [35]. It shows only the factors that are significant at the 95% confidence interval. From fig. 9 shows that significance effect upon efficiency has the control factors: pH, temperature and Particle Size. It is clearly that the variables considered in this investigation play an important role in the adsorption studies of dye removal since each variable has a significant

contribution to the dye removal. A main effect occurs when the mean response changes across the levels of a factor. The main effect plots are used to plot data means when multiple factors are involved in the system and also to compare magnitudes of marginal means [36]. The points in the plot are the means of the response variables at the various levels of each factor, with a reference line drawn at the grand mean of the response data. Grand mean is the mean of all observations, as opposed to the mean of individual variables. The line drawn across the plot (center line) represents the grand mean. From fig. 9 it is clearly that the grand mean of the response falls at around maximum dye removal. If the slope is close to zero, then the magnitude of the main effect would be small. The main plot (fig. 9) showed that interaction of Temperature played major role and also Particle Size - Temperature factors interacted strongly with other factors indicating predominant influence in adsorption capacity. Additionally, the factor Temperature appears to have a greater effect on the response, as indicated by a steeply slope.

Effect of Residual plot

In addition, normal probability plots and residual plots are compared to the plots with the fitted values based upon the removal efficiency of BBY onto AHCF are illustrated in Fig. 10.

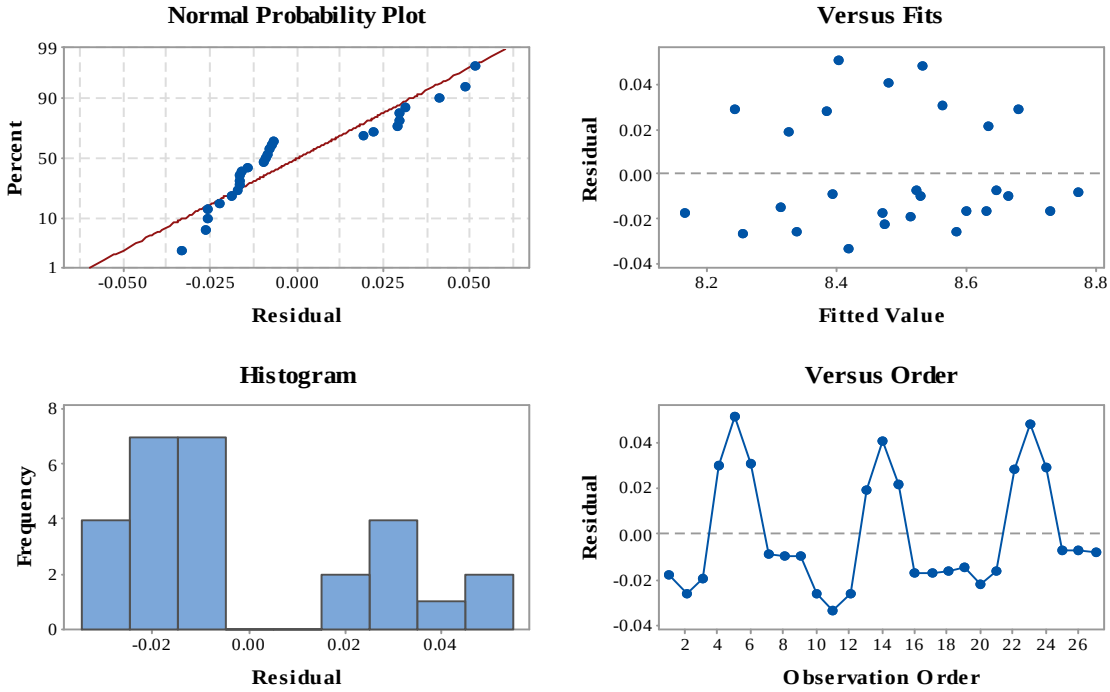

Fig. 10 Residual plots for BBY adsorption

Normal probability plot is a suitable graphical method for judging the normality of the residuals. As seen in residual plot the normality assumption is relatively satisfied as the points in the plot are clustered around line indicates that the error terms are approximately normal. Thus, our assumption of normality is valid [30]. The reliability of the model is also examined with the plot of residuals Vs fits in fig. 10 (b). It shows the error terms against the fitted values, the number of increasing or decreasing points is significantly close; patterns of increasing residuals and increasing fits are similar positive and negative residuals are scattered in the same range. On the same graph we see the clear cyclic pattern among the error terms indicating that they are violating the assumption of independence of error. The error terms are not independent. As a result, Figure shows that the model is adequate to describe adsorption of dye by response Factorial design for AHCF. The residuals are the differences between experimental and predicted values of q_e. From fig.13 shows the normal probability plot, variation of the fitted values, and histogram of the residuals for adsorption of dye. It is obvious that experimental runs present a normal distribution. The residuals are not linked to the estimated response. This is easily checked by plotting the residuals Vs estimated values. Note that no pattern should be seen in residual plot. The histogram distribution of q_e indicated that the data points larger than 2 are considered an outlier. The corresponding data points, which have values larger than 2, are between −0.75 to −0.25 and 0.25 to 0.75 in histogram plot. In fig. 11d again re-emphasizes the normality assumption. The sample size is just 26.

Effect of Pareto chart

A Pareto chart can be constructed by segmenting the range of the data into groups. The relative importance of the effects to compare the relative magnitude and the statistical significance of both main effects and their interactions is also observed on the Pareto chart. The individual effects of various parameters as well as their interactions can be discussed from the Pareto chart illustrated in the fig. 11. The length of each bar is proportional to the absolute value of its associated regression coefficient. The student t-test is performed to determine whether the calculated effects are significantly different from zero, these values for each effect is shown in the Pareto chart by horizontal columns [37]. For the 95% confidence level and eight degrees of freedom, the t-value is 2.09. As shown in fig. 11, some values are positioned around a reference line, but these values are not significant factors. The values that exceed a reference line, i.e., those corresponding to the 95% confidence interval, are significant values [38]. The main factors (A, B and C) and interaction effect BC that extend beyond the reference line are significant at the level of 0.05. The temperature represented the most significant effect on q_e. The pH (A), temperature (B), Particle size (C) has greater effects on q_e. While, except for the interaction effect between AB, AC and ABC have smaller effect and are statistically not significant at 95% confidence level.

Effect of normal probability plots

To identify the real effects, a normal probability plot is used. One point on the plot is assigned to each effect. According to the normal probability plots, the points which are close to a line fitted to the middle group of points represent those estimated factors that do not demonstrate any significant affect on the response variables. Points far away from the line likely represent the "real" factor effects [39]. The linear plot of Percent Vs Standardized effect showed that the adsorption of different dyes using the Normal probability plot is observed from the adsorption experiments carried over by using AHCF of three different particle sizes namely 100, 150 and 250 BSS mesh numbers is agitated with Bismarck Brown of known concentrations at 300, 310 and 320K. From fig. 12 shows the normal probability plot of the standardized effects to evaluate the significance of each factor and its interactions on adsorption capacity (q_e).

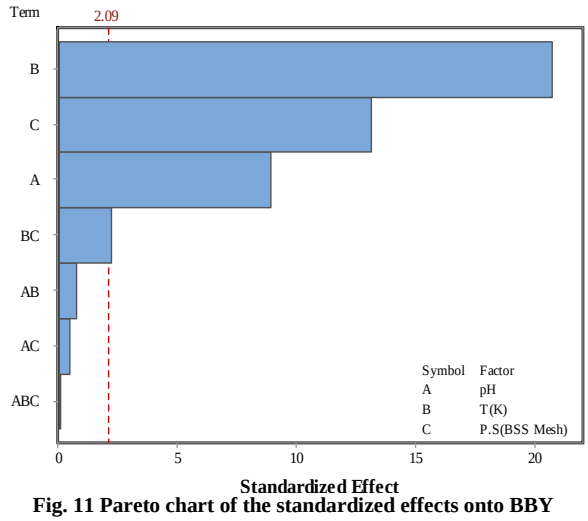

Fig. 11 Pareto chart of the standardized effects onto BBY adsorption

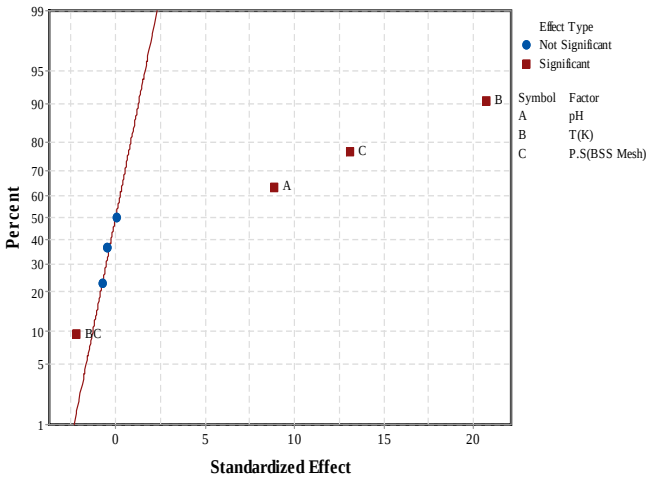

Fig. 12 Normal probability plot of standardized effects for BBY adsorption

Normal probability plot could be separated into two regions, the region with percent above 50% where the factors are indicated positive coefficients effect and the region with percent below where the factors are indicated negative coefficients effect. All these factors and interactions denoted as a circle are not significant and the effects shown as a square is significant [26]. The main factors (A, B, and C) are away from the straight line and are therefore considered to be "real". A, B and C on the right has a positive effect for all the dye adsorption. From fig. 12 the Temperature (B) has largest effect because its point lies farthest from the line. The second important factor is Particle Size (C) which is more significant than A (pH). These results confirm the previous Pareto chart analysis and the values of Table 7 The calculated data from the model predicted values [35]. The normal probability plot of residuals for q_e showed how closely the set of observed values followed the theoretical distribution. Generally, experimental points are reasonably aligned, suggesting a normal distribution. The selected model adequately described the observed data, explaining approximately 96.6% (due to R^2=0.966) of the variability of adsorption capacity (q_e).

Effect of Contour Plot

The effect of variables is analysed and plots are obtained to assess the response of each factor graphically. The response of certain factors is function that describes how the response moves as the level of those factor changes, when the other factors are fixed at their optimum levels. From figs. 13 to 15, it can be observed that each of the three variables used in the present study has its individual effect on adsorption.

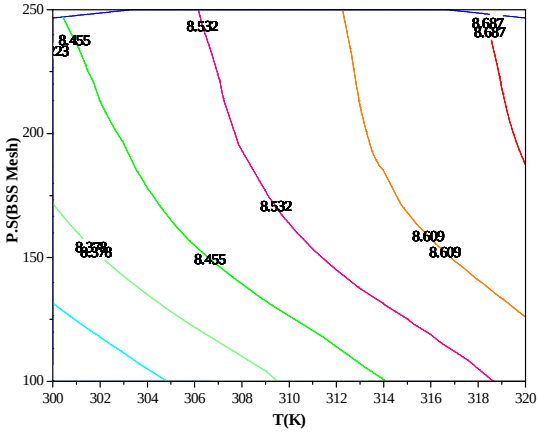

Fig. 13 Contour plot of BBY adsorption showing effect of T (K) and Particle Size

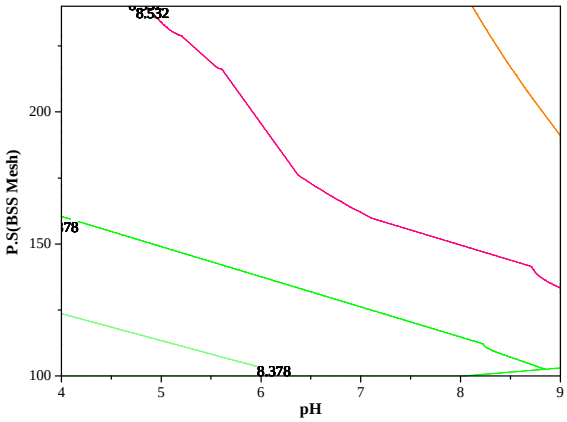

Fig. 14 Contour plot of BBY adsorption showing effect of pH and Particle Size

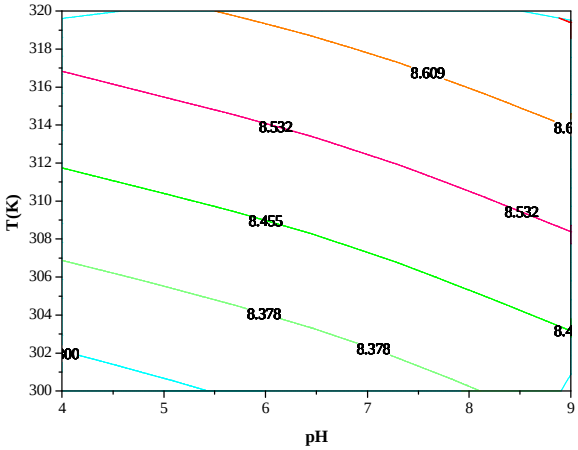

Fig. 15 Contour plot of BBY adsorption showing effect of pH and T(K)

From the contour plots, it has been found that there is a gradual increase in adsorption of dyes with increase in temperature from the lower level 300K (Coded value -1) to the higher level 320K (Coded value +1). Similarly, the adsorption increases with respect to the particle size of AHCF from 100 to 250BSS mesh numbers (Coded value -1 to +1). It is also revealed that the cationic dye would have small change to adsorption with respect to pH change. The pH level selected for this study is 4 to 9 (coded value -1 to +1). The result obtained by adapting factorial design in the study of adsorption of dye on the AHCF proves, Process temperature and particle size has an adverse effect on the response for AHCF. Other parameter like pH affected the process of adsorption significantly. The experimental values and the predicted values of Factorial design model are in close agreement with quadratic regression >99%. From the contour plots figs. 13 to 15, it is revealed that temperature at 320K and carbon particle size of 250 BSS mess number highest level of absorption. Similar types of results are observed by [40].

CONCLUSION

The statistical design of the experiments combined with is applied in optimizing the conditions of maximum adsorption of the BBY dye onto AHCF. The optimized conditions of pH, Particle size and Temperature with fixed initial concentration of 20 mg/L for dye adsorption are found at 7-9, 250 BSS mesh and 320 K, respectively which correspond to the maximum adsorption capacity of BBY. Common statistical tools such as ANOVA and F-test are used to define the most important process variables affecting the efficiency of dye adsorption process. The use of factorial design allowed for identification of the most significant factor under test conditions. Temperature and particle size is the greatest influence on the amount of dye removal. It demonstrated a significant interaction between Temperature and particle size. This interaction had more influence on dye removal than did the other interactions (pH-Particle size, pH-Temperature, pH-Particle size-temperature) had a positive influence on dye

removal, but the interaction factor Particle Size and temperature shows negative effect is the validity of this study is limited to pH between 4 - 9, particle size 100 - 250 BSS mesh and temperatures between 300 - 320 K. Findings indicated that the waste materials of Areca husk can be used as a potential adsorbent for the uptake of the dyes from aqueous solution is economical than any other commercially available activated carbon.

Acknowledgements
The author is grateful to Kumaraguru college of Technology, Coimbatore (Tamil Nadu), India for providing the necessary research facilities.

REFERENCES

[1] T Robinson, G McMullan, R Marchant, P Nigam, *Bioresource Technology*, **2001,** 77(3), 247-255.
[2] A Baban, A Yediler, NK Ciliz, *Clean*, **2010**, 38, 84-90.
[3] KV Radha, V Sridevi, K. Kalaivani, *Bioresource Technology*, **2008**, 100(2), 987-990.
[4] D Rajkumar, BJ Song, JG Kim, *Dyes and Pigments*, **2007**, 72(1), 1-7.
[5] J Chen, M Liu, J Zhang, Y Xian, L. Jin, *Chemosphere*, **2003**, 53(9), 1131-1153.
[6] W Konicki, D Sibera, E Mijowska, ZL Bielun, U Narkiewicz, *Journal of* Colloid *and* Interface Science, **2013**, 398, 152-160.
[7] M Visa, C Bogatu, A Duta, *Applied Surface Science*, **2010**, 256(17), 5486-5491.
[8] S Banerjee, MC Chattopadhyaya, *Arabian Journal of Chemistry***, 2015**(In press).
[9] S Hajati, M Ghaedi, F Karimi, B Barazesh, R Sahraei, A Daneshfar, *Journal of Industrial and Engineering Chemistry*, **2014**, 20(2), 564-571.
[10] KS Hameed, P Muthirulan, SM Meenakshi, *Arabian Journal of Chemistry*, **2014** (In press).
[11] M Ghaedi, A Ansari, R Sahraei, *Spectrochim Acta A Molecular Biomolecular Spectroscopy*, **2013**, 114, 687-694.
[12] HM Mozammel, O Masahiro, SC Bhattacharya, *Biomass and Bioenergy*, **2002**, 22(5), 397-400.
[13] K Srinivasan, B Sankar Rao, K Periasamy, A Ramadevi, *Journal of Indian Council of Chemists*, **1988**, 2, 61-64.
[14] S Rangaraj, A Banumathi, B Murugasan, *Indian Journal of Chemical Technology*, **1999**, 6(5), 1-4.
[15] GN Manju, C Raji, TS Anirudhan, *Water Research*, **1998**, 32(10), 3062-3070.
[16] EK Lee, JR Mirasol, J Cordero, JJ Rodrigrez, *Carbon*, **1993**, 31(1), 87-95.
[17] DK Singh, J Lal, *International journal of Environmental Health care*, **1992**, 34, 108-113.
[18] K Gregova, N Petrov, V Minkova, *Journal* of *Chemical Technology* and *Biotechnology*, **1993**, 56(1), 77-82.
[19] J Hu, Z Song, L Chen, H Yang, J Li, R Richards, *Journal of chemical and engineering data*, **2010**, 55(9), 3742-3748.
[20] M Mohammadi, AJ Hassani, AR Mohamed, GD Najafpour, *Journal of chemical and engineering data*, **2010**,55(9), 5777-5785.
[21] S Coruh, S Elevli, *Global Nest Journal*, **2014**, 16(2), 339-347.
[22] BD Cullity, Elements of X-ray Diffraction, *Addison-Wesley company publishing Inc.* **1978.**
[23] C Namasivayam, D Kavitha, *Microchemical Journal*, **2006**, 82(1), 43 - 48.
[24] C Namasivayam, D Kavitha, *Separation Science and Technology*, **2004**, 39(6), 1407-1425.
[25] K Ramesh, V Nandhakumar, *International Journal of Current Research in Chemistry and Pharmaceutical Sciences*, **2014**,1(4), 15-19.
[26] N Ozbay, AS Yargic RZ Sahin, E Onal, *Journal of chemistry*, **2013**, 1-13.
[27] LS Lima, MDM. Araujo, SP Quinaia, DW Migliorine, JR Garcia, *Chemical Engineering Journal*, **2011**, 166(3), 881-889.
[28] W Navidi, Statistics for engineers and scientist, *McGraw-Hill Companies, Inc*., New York **2008.**
[29] D Kavak, *Journal of Hazardous Materials*, **2009,** 163(1), 308-314.
[30] B Ucar, A. Guvenc, U. Mehmetoglu, *Hydrology Current Research*, **2011**, 2(2), 1-8.
[31] BB Kar, Y Swamy, BVR Murthy, *Hydrometallurgy*, **2000,** 56(3), 387-394.
[32] BP Singh, L Besra, S Bhattacharjee, *Colloids and Surfaces A Physicochemical and Engineering Aspects*, **2002**, 204(1-3), 175-181.
[33] R Gottipati, S Mishra, *Chemical Engineering Journal*, **2010**, 160(1), 99-107.
[34] K Adinarayana, P Ellaiah, B Srinivasulu, R Bhavani Devi, G Adinarayana, *Process Biochemistry*, **2003**, 38(11), 1565 - 1572.
[35] NT Ghani, AK Hegazy, GA El-Chaghaby, EC Lima, *Desalination*, **2009**, 249 (1), 343-347.
[36] F Geyikci, *ACTA Geodyn Geomater*, **2013**, 10(3), 363-370.
[37] V Ponnusami, V Krithika, R Madhuram, SN Srivastava, *Journal of Hazardous Materials*, **2007,** 142(1-2), 397-403.
[38] T Mathialagan, T Viraraghavan, *Environmental Technology*, **2005,** 26(5), 571-579.
[39] K Palanikumar, JP Dawim, *Journal of Materials Processing Technology*, **2009**, 209(1), 511-519.

[40] G Annadurai, S Mathalaibalan, T Murugesan, *Bioprocess Engineering*, **1999**, 21, 415-421.